Sea level rise will change estuarine tidal energy: A review

Khojasteh, Daniel; Lewis, Matthew; Tavakoli, Sasan; Farzadkhoo, Maryam; Felder, Stefan; Iglesias, Gregorio; Glamore, William

Renewable and Sustainable Energy Reviews

DOI:
10.1016/j.rser.2021.111855

Published: 01/03/2022

Tidal power and sea level rise in estuaries: A review

Danial Khojasteh [a,*], Matthew Lewis [b], Sasan Tavakoli [c], Maryam Farzadkhoo [a],

Stefan Felder [a], William Glamore [a], Gregorio Iglesias [d, e,*]

[a] *Water Research Laboratory, School of Civil and Environmental Engineering, UNSW Sydney, NSW 2052, Australia*

[b] *School of Ocean Sciences, Bangor University, Menai Bridge LL59 5AB, UK*

[c] *Department of Infrastructure Engineering, The University of Melbourne, Parkville, 3052, VIC, Australia*

[d] *School of Engineering and Architecture & MaREI, Environmental Research Institute, University College Cork, College Road, Cork, Ireland*

[e] *University of Plymouth, School of Engineering, Marine Building, Drake Circus, Plymouth, PL4 8AA, United Kingdom*

[*] Corresponding authors
Email addresses: danial.khojasteh@unsw.edu.au; m.j.lewis@bangor.ac.uk; stavakoli@student.unimelb.edu.au; maryam.farzadkhoo@unsw.edu.au; s.felder@unsw.edu.au; w.glamore@wrl.unsw.edu.au; gregorio.iglesias@ucc.ie

Abstract

Climate change induced sea level rise (SLR) will affect tidal dynamics and the associated processes, including the tidal energy resource of estuaries. A hierarchy of factors influencing the future tidal energy resource is proposed based on their relevance to SLR. Primary factors, including tidal prism, tidal range, tidal currents, and tidal asymmetry, are directly affected by SLR, whereas secondary factors (e.g., sediment transport) are affected by SLR through changes in primary factors. Finally, tertiary factors (e.g., shifts in estuarine shape/landform) are mediated by primary and secondary mechanisms. Related knowledge gaps are identified in existing literature, including the effects of SLR on different types of estuaries. Previous research suggests different responses in tidal energy to SLR for different estuary types. For instance, SLR may cause tidal ranges or currents to strengthen or weaken, depending on estuarine shape and boundary conditions (e.g., presence or absence of levees and adjacent low-lying areas). The lack of overarching knowledge on the subject is often hindered by the highly local character of previous studies. Comparative studies encompassing different regions and types of estuary are recommended to address the existing knowledge gaps and provide insights for policymakers and stakeholders in tidal energy projects. The interaction of estuarine processes, that underpins SLR-induced changes to tidal energy resource, can alter the available resource within a renewable energy development's operational lifetime (~120 years). Until these knowledge gaps have been addressed, long-term management decisions associated with harnessing the full potential of tidal energy schemes in estuaries should be made with caution.

Highlights

- A review of research regarding tidal energy and sea level rise (SLR) in estuaries is provided.
- Knowledge gaps remain related to the impacts of SLR on tidal energy distribution and location of hotspots.
- A hierarchy of factors influencing the tidal energy resource is proposed based on their relevance to SLR.
- Estuarine tidal energy may be affected by SLR through changes in tidal prism, range, current, asymmetry, and sediment dynamics.
- SLR have planning and management implications for existing and future tidal stream and tidal range energy schemes.

Keywords: Tidal energy, tidal dynamics, tidal stream turbine, tidal barrage, renewable energy, climate change.

Word Count: 6945

1 Introduction

There is broad consensus that estuaries are among the most valuable natural environments worldwide due to their ecological and socio-economic services [1-3]. Estuarine environments are important for primary production, flood and storm protection, recreation, navigation, and energy generation [4-7]. For these reasons, human settlements established themselves in estuarine areas, and nowadays, 22 out of the 32 largest cities in the world lie adjacent to estuaries [5, 8, 9].

Estuaries are ideal locations for extracting tidal energy due to their high tidal ranges, strong tidal currents, and proximity to energy consumption areas and grid connection points, which reduces the transmission losses and therefore the cost of energy [6, 10-12]. In recent years, tidal energy has received increased interest as a form of clean energy that could contribute to alleviating the global energy crisis and mitigating the impacts of climate change [13-15]. Indeed, tidal energy is one of the most promising renewable energy resources given its advantages including that it is highly predictable, cost-effective, presents high load factors (water is approximately 800 times denser than air), and has limited environmental impacts [16-25]. Therefore, the efficient exploitation of this underutilised resource can increase the future share of renewable energies in the energy mix and thus, meeting the ambitious decarbonisation targets worldwide [19, 26-32].

Implementing tidal energy solutions requires a thorough understanding of estuarine hydrodynamics. The hydrodynamics are governed by several driving forces (tides, winds, river inflows, storm surges, etc.), intrinsic fluid properties (e.g., density, viscosity), estuarine geometry and bathymetry (e.g., length, depth, mouth condition, intertidal areas), as well as frictional effects (e.g., bed roughness) [33-36]. These elements play an important role in the distribution of tidal energy (Fig. 1). There are two common approaches to exploit tidal energy [37] including (a) tidal barrages, which span the entire width of the estuary, impound upstream flow, and create a head difference [38]; or tidal stream turbines, which harness the kinetic energy of the tidal currents [39, 40].

As estuaries are transition zones between the open ocean and rivers, they are typically surrounded by low-lying coastal areas and are highly vulnerable to climate change driven sea level rise (SLR) [33, 41-43]. The prediction of SLR depends on several factors including which Representative Concentration Pathway (RCP) emission scenario is considered [44]. The latest report by the Intergovernmental Panel on Climate Change (IPCC) projected a SLR of 0.29–0.59 m for RCP2.6, and 0.61–1.10 m for RCP8.5 by 2100, relative to 1986–2005 levels [44]. However, significant uncertainties exist regarding the contribution of the Greenland and Antarctic ice sheets to future global mean SLR [45]. For instance, a recent study suggests a SLR of 0.30–0.65 m for RCP2.6 and 0.63–1.32 m for RCP8.5 by 2100 [46], while other researchers predict a SLR of over 2 m for RCP8.5 scenario by 2100 [45, 47].

Accelerating SLR can alter estuarine tidal dynamics (e.g., tidal prism, tidal range, tidal currents, and tidal asymmetry) mainly through the modification of the geometry and bathymetry (water depth, entrance condition), as well as frictional and tidal resonance effects [35, 48] (Fig. 1). Further, anthropogenic activities (e.g., land reclamation, construction of levees or entrance training walls) can also modify estuarine tidal dynamics. Figure 1(a) depicts a historic estuarine system with its driving forces, natural roughness, and water storage areas. Figure 1(b) shows the present-day condition of the same estuary, where SLR and anthropogenic activities have led to further changes in tidal dynamics. Figure 1(c) illustrates a future condition of the system, where climatic factors (e.g., altered precipitation), extended human activities, and larger SLR will likely bring about significant variations in tidal characteristics. In particular, SLR will likely change the spatial and temporal distributions of tidal energy and thereby the optimum locations for tidal energy farms in estuaries [49-51].

Although previous estuarine tidal dynamics and SLR studies have shown alterations in tidal range [52, 53], current velocity [33], asymmetry [54], and prism [55], significant knowledge gaps remain with regards to variations in estuarine tidal energy under SLR (e.g., distribution, location of hotspots). Existing studies are typically localised [49, 56] due to the need to resolve a wide range of spatial scales (from offshore forcing to high-resolution of estuarine processes and responses [57, 58]). Therefore, a thorough understanding regarding the complex influence of SLR on estuarine tidal energy (or power) is currently lacking in order to better develop sustainable and green energy plans, protect tidal energy infrastructures, and ensure security of energy generation. Given the need to resolve the tidal energy resource for the lifetime of a deployment (~120 years), within the yield calculation of like cost-benefit assessment (so called Levelized-Cost-of-Energy), hypothesised changes to the tide under SLR, and the lack of global tidal models at resolutions necessary to resolve all estuaries (i.e., spatial scales < 1 km); there is a need to review and quantify potential changes to estuary tidal energy resource within estuaries under SLR.

This review aims to address the knowledge gap regarding the effects of SLR on estuarine tidal energy and assist policy makers and stakeholders in designing holistic and evidence-based management strategies for future tidal energy development under accelerating SLR. To this end, Section 2 presents an introduction on tidal stream energy in different estuaries and how tidal stream energy distribution and the location of hotspots are likely to be affected by SLR. Section 3 provides a detailed overview of estuarine tidal range energy schemes and how SLR will likely influence their operation. Section 4 offers a critical discussion regarding the absence of a systematic study considering the variations in tidal energy for different estuary types under SLR, detailing the complex feedback loops between estuarine processes under SLR and, where appropriate, presenting directions for future research and management. Finally, conclusions are drawn in Section 5.

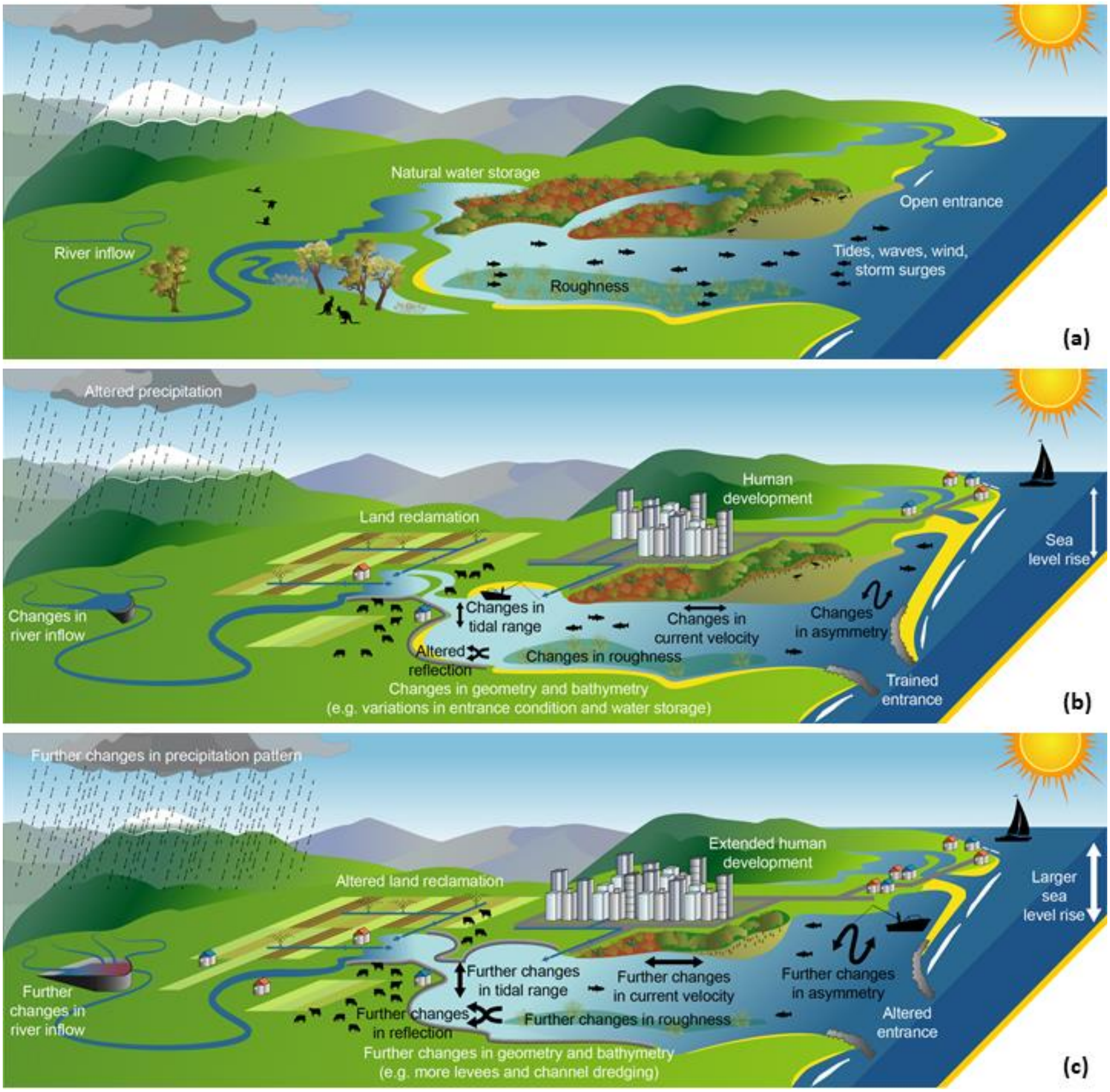

Fig. 1. Conceptual schematics of an estuarine system in (a) historic, (b) present-day, and (c) future conditions, indicating estuarine driving forces as well as changes in estuarine processes due to climate change induced SLR and human activities.

2 Tidal stream energy and sea level rise

2.1 Tidal currents, power density, and in-stream turbines

The gravitational forces between the Earth, the Moon, and the Sun as well as the Earth's rotation create tides that vary on regular time scales (i.e., from daily to interannual) [48]. In an estuary, the rise and fall of the tide induces a certain volume of water (the tidal prism) to enter and leave an estuarine system, causing the water to move horizontally and generating tidal currents (streams) [59]. Tides can be also influenced by various factors (in addition to rotational and gravitational forces) including estuarine geometry (e.g., length, depth, entrance condition), bed/banks roughness (e.g., vegetation distribution), other driving forces (e.g., interaction with waves and river inflows), and anthropogenic activities (e.g., dredging, protective walls) (see Fig. 1) [33-35, 60]. Any changes to these physical/environmental factors can alter tides which, in turn, can modify tidal currents [35]. Generally, tidal streams are strongest around the peaks of low and high tides (spring tides, corresponding to new or full phases of the Moon).

A common approach to extract power from tidal currents is to use tidal stream turbines, which harness the kinetic energy of the moving water to power turbines by mounting a resistance to the flow over the area swept by the turbine blades [39, 61, 62]. In practice, only a portion of the total available kinetic energy flowing through the turbine can be captured [63] due to mechanical losses in the turbine and Betz Law [59, 62], which is estimated as:

$$P = \frac{1}{2} C_p \rho V^3 \qquad (1)$$

where P [W/m^2] is the power density per square meter swept by the turbine rotor, C_p is a power coefficient, ρ [kg/m^3] is the density of water, and V [m/s] is the magnitude of the stream velocity.

To date, 1st, 2nd, and 3rd generations of tidal stream energy technologies are often feasible in areas with peak spring tidal currents exceeding 2.5, 2, and 1.5 m/s, respectively, and water depths of 25-50, > 25 m, > 25 m (with a shift towards all water depths), respectively [57, 64]. Based on the turbine characteristics, these technologies can be generally classified into six different groups [65-67], as illustrated in Fig. 2. Horizontal axis turbines convert the kinetic energy of the streams to electricity with the turbines mounted on a horizontal axis (C_p = 0.4-0.45 at the optimal tip speed ratio [68]) (Fig. 2(a)). Vertical axis turbines are similar to horizontal axis units but the turbines rotate around a vertical axis (C_p = 0.4 at the optimal tip speed ratio [68]) (Fig. 2(b)). These turbines are less common in comparison to their horizontal axis counterparts. Oscillating hydrofoils encompass hydrofoils attached to an oscillating arm, which are displaced up and down by the currents (Fig. 2(c)). This oscillatory (rather than rotary) motion is then transformed to electricity through a hydraulic system, which is connected to the arm. These tidal energy converters are easier to manufacture and can be employed in shallow water sites [69]. Venturi or enclosed tips are funnel-like devices that help concentrate and accelerate the currents that pass a turbine enclosed within the system (Fig. 2(d)). Archimedes screws include a cylindrical pole surrounded by a helical surface which can power a turbine when currents pass through the spirals (Fig. 2(e)). Tidal kites are tethered to the bed and fly in the tidal streams to increase the speed of currents flowing through their small turbines (Fig. 2(f)). These tidal energy converters can operate in low velocity currents [70].

Horizontal and vertical axis turbines may also be used in floating configurations. Floating turbines are better able to exploit the greater flow speeds near the surface. They have typically smaller diameters than their bottom-fixed counterparts and may be of interest in areas where water depth is limited [24]. One aspect to consider in deciding between floating and bottom-fixed turbines is their impact on estuarine hydrodynamics, which is different, especially in the vicinity of a tidal stream farm [40].

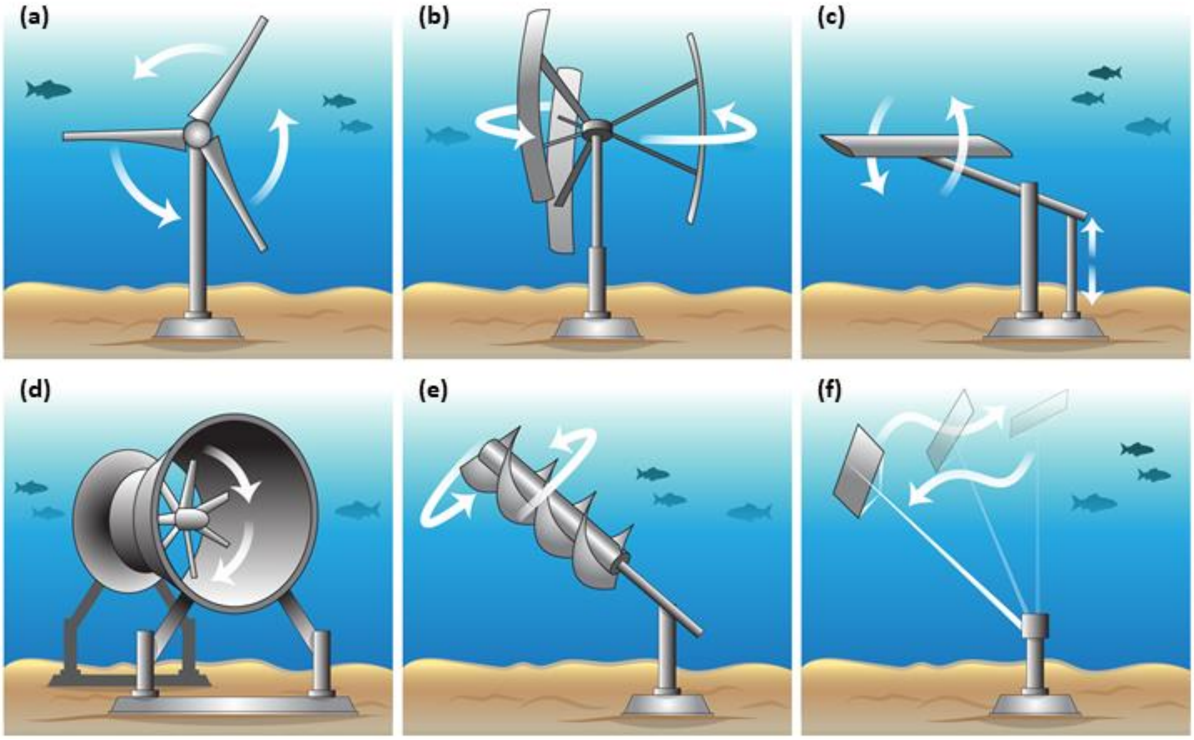

Fig. 2. Various types of tidal stream energy devices including (a) horizontal axis turbine, (b) vertical axis turbine, (c) oscillating hydrofoil, (d) venturi (or enclosed tip) turbine, (e) Archimedes screw, and (f) tidal kite.

2.2 Sea level rise and distribution of tidal stream energy and hotspots

In estuaries, any variation in mean sea level is associated with nonlinear changes in tidal characteristics [34], depending on driving forces, estuarine shape (e.g., length, width, depth, entrance condition, availability of intertidal areas), and roughness (e.g., bed/banks friction) [33, 35] (Fig. 1). As SLR alters the water depth, it can modify the tidal prism and tidal range and consequently the distribution of current velocities and stream power. As discussed in detail in [34, 35, 48], there are various mechanisms by which SLR can induce changes in the tidal dynamics, including changes in frictional effects, tidal resonance, and the location of amphidromic points (also called nodal points – locations with zero tidal amplitudes) [33-35, 48, 52, 53]. Further, as SLR brings about changes to tidal prism and current velocity distribution, it can influence the sediment transport dynamics (i.e., geomorphology) [71] or water quality (e.g., salinity) [72, 73] of an estuarine system. Over various time scales and through complex and interconnected feedback loops under SLR, the adjustments in estuarine geomorphology (e.g., changing estuarine shape) and water quality (e.g., changing vegetation distribution with a different roughness) can lead to further variations in tidal energy dynamics. Here, the influence of altered geomorphology and friction as well as displaced amphidromic points under SLR on tidal stream power and hotspots are discussed in detail, and the effect of SLR on tidal resonance is presented in Section 3.

SLR can induce nonlinear changes to estuarine tidal prism and tidal range. SLR can increase the cross-sectional flow area at the mouth, bring about an increase in the exchange volume in and out of the entrance over a tidal cycle, and reduce the effective bed friction (Fig. 3) [35]. For instance, by considering fixed inlets, it is predicted that the tidal prisms of the Perdido and Choctawhatchee Bays along the Northern Gulf of Mexico would increase by 52% and 44% under 0.46 m of SLR, respectively [55]. However, in the nearby St. Andrew Bay, SLR decreases the tidal prism by 1% due to a reduction in its planform area [55]. The distribution of current velocities and power will likely vary in these systems. Further, the New Jersey coastlines facing the Atlantic Ocean would experience a decrease in their tidal power density, while the Delaware Bay in the same region would undergo a tidal power amplification under 1 m of SLR [49].

In estuaries with restricted entrances, only a limited volume of water can flow in and out of the system with tidal dampening at the entrance [33]. The tidal prism of idealised estuaries with highly restricted entrances can increase by up to 15% per meter of SLR [33]. Further, in estuaries with upstream bridges, levees (dykes), or weirs, the propagating tidal waves would reflect seaward, leading to a tidal range amplification. This phenomenon is most evident in 1/3 of the most upstream part of the estuarine system [74]. These increases in tidal range, in turn, can modify the distribution of flood and ebb velocities, and hence, the tidal asymmetry (i.e., difference between the strength of the ebb and flood velocities) [33, 54], and power density [49]. The altered tidal asymmetry can also shift the location of optimal sites for tidal energy extraction as it is beneficial to exploit sites with tidal symmetry (i.e., equal strength of the ebb and flood velocities) and not with tidal asymmetry (i.e., unequal strength of the ebb and flood velocities) [75]. This variation can have adverse or beneficial effects on the location of hotspots for tidal energy harvesting. For instance, a SLR of 1 m would eliminate a few energy hotspots across the New Jersey coastlines but create new ones in the nearby Delaware Bay [49, 50]. Altered tidal asymmetry is also significant in determining the geomorphology of an estuary as a flood dominated system promotes net landward sediment transport, whereas an ebb dominated system results in net seaward transport [76]. The SLR-induced geomorphic variation occurs over longer time scales, and can bring about changes in the distribution of tidal currents through ongoing feedback loops [35]. To illustrate, if over time, the shape of an estuary shifts from prismatic to converging or vice versa (e.g., Yangtze River estuary [77]), the estuary would experience a likely increase in its tidal stream velocity and power [78]. Further, it is estimated that short and/or prismatic estuaries are likely to experience significant variations in their tidal stream velocity and power distributions under SLR in comparison to long and/or converging estuaries [78]. As such, if SLR-induced geomorphic variations and/or anthropogenic activities alter the shape of an estuarine system, the tidal current distribution and power density will change substantially.

The tidal prism is potentially larger in estuaries with vast low-lying floodplain where intertidal areas can be inundated under SLR, in comparison to those where overland flooding is prevented via protective structures (e.g., levees and dykes) [35]. If intertidal areas are inundated under SLR, the new shallow zones will add natural water storage and friction, and tides are likely attenuated due to the dissipative effects of these areas [41, 53]. For instance, 2 m of SLR is predicted to increase the tidal current velocity in the Grand (102%), Weeks (39%), and Apalachicola (63%) Bays, but a decrease in the northern Chandeleur Islands in the same region due to the barrier island being overtopped [79]. SLR potentially decreases the tidal range in the Delaware Bay if the shallow tributaries are allowed to be inundated but increases if protective measures are adopted [53]. The changes in tidal range and prism and consequently stream velocities under SLR by activating intertidal areas can alter the distribution of tidal power density and hotspots for tidal energy development. These changes, in turn, can influence the hydroperiod (i.e., frequency, depth, and duration of inundation), which is a key factor in controlling the vegetation distribution of intertidal wetlands, such as mangrove species [43, 80], leading to altered bed friction as new vegetation communities have different roughness.

SLR can also shift the location of the amphidromic points (Fig. 3), generating spatially variable fluctuations in the distribution of tidal streams and energy [34, 48, 52]. Amphidromic points occur at $\frac{(2m+1)\lambda}{4}$ from the end of the estuary, where λ is the wavelength ($\lambda = T\sqrt{gh}$, where T and h are tidal period and water depth, respectively). For instance, in the Chesapeake Bay, SLR shifts the amphidromic points away from the head and amplifies the tidal range [81]. For this estuary, SLR increases the water depth, decreases bed friction, increases the wavelength, and thereby, moves the amphidromic point towards the mouth, and increases the tidal range particularly in the upstream reaches [52] (Fig. 3). Likewise, the influence of SLR on tidal dynamics is more evident in the upper part (85 km from the mouth) of the Gironde River estuary, where 1 m of SLR increases the tidal range and tidal current velocity [82]. These variations result in an uneven distribution of tidal currents and bring about significant changes in tidal stream energy and hotspots within an estuarine system, posing a significant challenge for sustainable management of estuaries and the security of energy generation under accelerating SLR, requiring further interdisciplinary research.

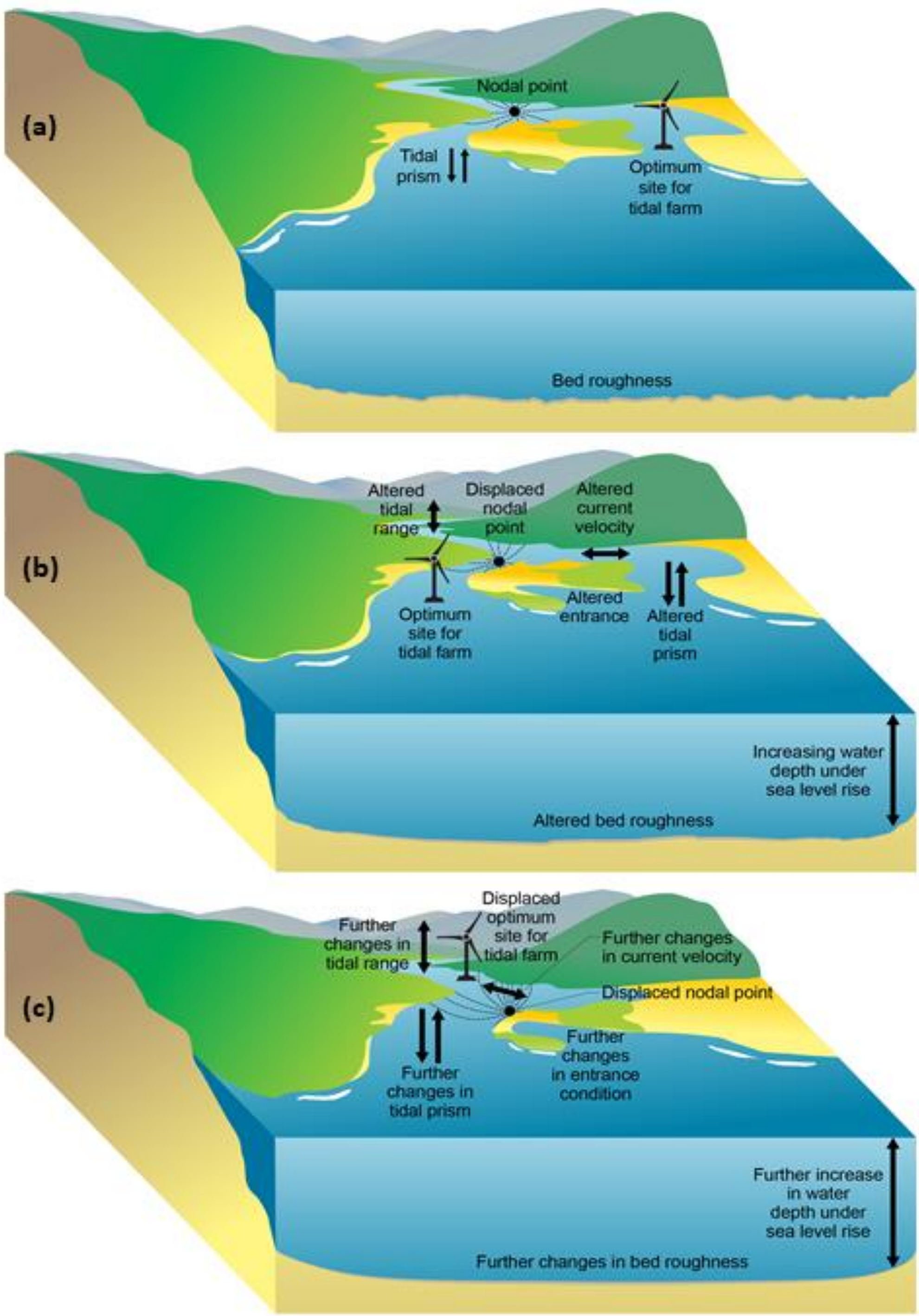

Fig. 3. Conceptual plots of an estuarine system in (a) historic, (b) present-day, and (c) future conditions. SLR can increase the water depth, reduce the frictional effects, adjust the geomorphology, modify tidal prism, move the amphidromic point(s), alter the tidal range, change the stream velocity, and displace the location of hotspots for tidal energy development.

3 Tidal range energy and sea level rise

3.1 Fundamentals of tidal range energy

Tidal range energy schemes are currently only considered economically viable if the mean tidal range is greater than 5 m, thus the amplitude of the major semi-diurnal lunar constituent, M2, larger than 2.5 m [83]. The present engineering approach for tidal range energy schemes in estuaries are barrages, which provide a barrier between the ocean and estuary. Sluice gates and turbines can artificially keep the water level at high or low tide, creating potential energy as the water level difference increases between the ocean and estuary during an ebbing tide, flooding tide, or both [11, 83].

The head difference across a tidal barrage can generate a maximum (i.e., neglecting energy losses) potential energy E_{max} [J] [84]:

$$E_{max} = \frac{1}{2}\rho g S(\Delta d)^2 \tag{2}$$

where g [m/s^2] is the gravitational acceleration, S [m^2] is the impounded wetted surface area, and Δd [m] is the head difference between the downstream and upstream sides of the impoundment and is often taken as the mean tidal range (difference between high and Low tide).

Two insightful reviews on tidal range energy schemes have been published recently [85, 86], and therefore, the present review directs the reader to these studies and instead focuses on the impact of future physical changes to energy resource in the remainder of this section, namely SLR.

The impact of SLR on global tides is known to be problematic [87], bringing about uncertainties in model parameterisation of the coastline [88] as well as temporal and spatial variability in tidal dynamics [89]. For instance, 10% changes to the major semi-diurnal lunar constituent appear possible in shelf sea systems [89]. It is indicated that in the UK, SLR appears to have minimal impact on resonant systems (Liverpool Bay with no significant change and a small decrease in the Bristol Channel) [90], whilst a recent study of the Irish Sea concluded significant changes to tidal dynamics in tidal energy regions and physical process interactions [58]. Given the interest in renewable tidal energy schemes, the observed and predicted SLR [91], as well as changes to shelf sea tidal systems [87, 89], the impact of SLR to tidal range resource appears an important issue to resolve [13].

3.2 Tidal range modifications under sea level rise

As highlighted above, SLR can modify estuarine tidal dynamics through various means, depending on estuarine geometry, driving forces, and boundary conditions. In the following sub-sections, different physical mechanisms are highlighted, including tidal resonance, shoaling, and funnelling. The interaction of these processes may influence the tidal range, and thereby the tidal range energy withing an estuarine system.

3.2.1 Tidal resonance

Tidal resonance occurs when basin length scales are such that the natural period of the basin matches the tidal wavelength (or product of) the wavelength. Tidal waves travel as a shallow-water wave and are controlled by the wave celerity $c = \sqrt{gh}$ (travel of highwater along an estuary). As such, the tidal resonance of an estuary can be modified not just by the estuary length but also by changes in water depth (i.e., dredging or SLR). Rising mean sea levels can shift an estuarine system closer to or further away from tidal resonance, leading to tidal amplification or dampening, respectively [48].

The impact of SLR on tidal resonance length scale for a simple, single harmonic tide of period 12.42 hours (i.e., the major semi-diurnal lunar constituent, M2) is demonstrated in Fig. 4(a), based on Merian's Formula (Eq. (3)) where the natural period (T) is a product of the mode of oscillation n (where n is number of nodes) and the wave celerity c, thus:

$$T = \frac{2nL}{\sqrt{gh}} \tag{3}$$

As T = 12.42 hours, the impact to L from 1 m and 2 m of SLR can be solved analytically. As such, if depth (h) is assumed to be uniform and constant, then $L \simeq$ 250 km; and as 1 m or 2 m of SLR are added then the resonant basin length (L) for an M2 tide increases by 1%. This effect is larger in shallower systems, e.g., 1.5% for 30 m and 4.5% for 10 m deep systems, as shown in Fig. 4(a). Therefore, estuaries close to resonance are most sensitive to length and/or depth variations [33, 34, 52, 92], and can experience a tidal range amplification in the upstream sections of the estuary [48], such as in the Bay of Fundy with a resonance period of 13.3 ± 0.4 hours [93]. In the Chesapeake Bay, which is a shallow system, 1 m of SLR has been shown to reduce the resonant period and shift the system closer to a resonant state [94]. In estuaries with large inundated floodplain areas, the tidal energy dissipation due to the flooding of low-lying lands can dampen or eliminate the tidal resonance effect [95]. As such, SLR-induced changes to resonance state of an estuarine system should be taken into account when designing long-term plans for construction of tidal range energy power plants.

3.2.2 Shoaling

In estuaries, shoaling is typically used to describe the physical process when tidal waves approach the shore. The reduction in water depth (h) results in an increase in wave height (H), relative to the deep water wave height (H_0), as wave energy flux per unit area and group velocity (EC_g) is reduced (for details, see [74]). Assuming no frictional losses or reflection at the head, the relative wave celerity (c/c_0) and wave number (κ) may estimate the analytical increase to wave height (H/H_0), as indicated in Eq. (4), where sub-script 0 denotes deep water wave properties (for details, see [96]):

$$\frac{H}{H_0} = \sqrt{\frac{EC_g}{E_0 C_{g0}}} = \sqrt{\left(\frac{c}{c_0}\right)\left(1 + \frac{2\kappa h}{\sinh 2\kappa h}\right)} \tag{4}$$

The shoaling process can also modify the tidal wave in long shallow inlets, and in extreme cases result in the phenomena of tidal bores [97, 98]. Here, the principles of Eq. (4) are used to explore the impact of SLR to tidal amplification due to shoaling, as illustrated in Fig. 4(b), where amplification of a 2 m amplitude M2 tide (period of 12.42hours) from an offshore water depth of 50 m is estimated for water depths that include SLR of 1 m and 2 m.

3.2.3 Funnelling

The concentration (funnelling) of tidal energy, as the tides propagate towards areas of reduced width, can also increase the tidal amplitude [99]. To estimate the increase in tidal amplitude, the continuity equation can be solved when the change in tidal wave celerity along the estuary length is included. Therefore, amplification is dependent on water depth ($\gamma = 1/h$) and shape, including width (β = $1/B$, where B is estuary width), which typically requires a computational model to solve. However, neglecting friction and assuming a constant water depth provides a simplified analytical solution called "Greens Law" [74]:

$$\frac{H}{H_0} = e^{(0.5+(\beta+\gamma)x)} \tag{5}$$

As such, Eq. (5) describes how the tidal height increases exponentially for exponentially decreasing width and depth. Assuming no geomorphic feedbacks, constant bathymetry of 50 m, 50 km length, and no frictional effects, the reduction in funnelling amplification of the tide is analytically solved in Eq. (5) for two SLR scenarios (1 m and 2 m). This example, shown in Fig. 4(c), highlights the decrease in the M2 tidal amplitude with increasing distance along estuary length (inland) via the effect of a SLR of 2 m.

The width of converging estuaries is often represented as an exponential function of the distance from the mouth along the estuary centreline as $B(x) = B_0 \exp(-x/L_c)$, where B_0 is the width at the estuary mouth, L_c is the width convergence length, and x is the distance from the mouth. The smaller values of L_c indicate stronger convergence. It is analytically demonstrated that tidal range can be amplified if $3\pi h\omega/8C_D U\kappa \gg L_c$, where C_D is the drag coefficient, U is the amplitude of width-averaged current velocity, and ω is tidal frequency [100, 101]. As such, strongly converging estuaries exhibit an increased chance of tidal range and energy amplification [78], such as in the upstream part of the Delaware Bay [81]. If, over various temporal scales, geomorphology of an estuarine system alters under SLR, the tidal range energy of the estuary would change significantly [78].

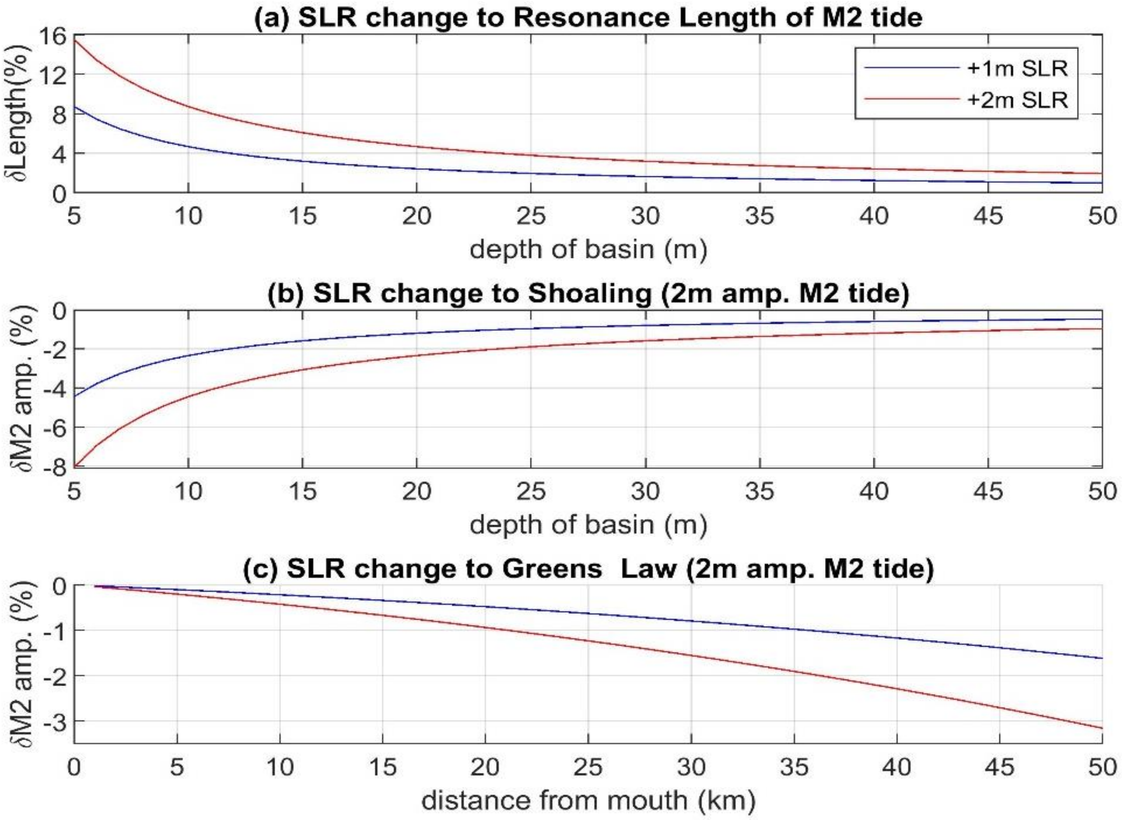

Fig. 4. Impacts of SLR on three main drivers of tidal amplification in estuaries with simplified analytical form including (a) resonance, (b) shoaling, and (c) Greens law. No geomorphic feedbacks were considered, water depth was assumed constant, and only a perfect M2 tide is applied.

3.2.4 Sea level rise influence on combined tidal amplification processes

Figure 4 indicates that as SLR increases the effective water depth, the tidal range amplification effects of shoaling and funnelling are reduced. However, Fig. 4 does not show the interaction of these physical processes, which shall be explored herein using a simplified 1D shallow water equation hydrodynamic model, assuming continuity (Eq. (6)) and momentum (Eq. (7)) equations. Here, the cross-sectional area of the estuary (A) is solved for an estuary width (B) and water level elevation (η), width-averaged current velocity (V) (for each discretised grid point (∂x)), water depth (h) and parameterised friction (drag coefficient, C_d). Such simplified 1D numerical model simulations have been shown to be effective in many estuaries, including the Bristol Channel – a site with a large tidal range resource [102].

$$\frac{\partial \eta}{\partial t} = -\frac{1}{B}\frac{\partial (AV)}{\partial x} \tag{6}$$

$$\frac{\partial V}{\partial t} = -\frac{\partial \eta}{\partial x} - \frac{C_d V^2}{(h+\eta)^{4/3}} \tag{7}$$

By assuming similar dimensions to the Bristol Channel, UK [102] where the estuary length is 170 km, a model was established with a discretisation of ∂x = 3.86 km, time-step of ∂t = 29 s, width of B = 140 km at mouth, converging at 44.8° with a constant water depth of h = 20 m, and an M2 tidal boundary amplitude of 1.5 m. Applying the 1D shallow water model of Eqs. (6, 7), numerical simulations of the impact of SLR were undertaken via combinations and interactions of the funnelling, shoaling and tidal resonance processes, as indicated in Fig. 5.

In Fig. 5, SLR was added to the model by increasing the water depth by 1 m and 2 m at the boundary. Fig. 5(a) indicates spatially varying changes to the tidal amplitude along the estuary length – but an overall decrease in tidal height. As is clear from Fig. 5, the impact of SLR is complicated, due to the combination of the three processes of tidal resonance, shoaling, and funnelling.

The results shown in Fig. 5 would differ for different estuary shapes, water depths, and assumptions (e.g., constant water depth, inflows, etc). This is demonstrated in Fig. 5 by the impact of increasing tidal amplitude of 10% at the model boundary (mouth), as depicted in Fig. 5(b) by the dashed lines. Indeed, a 10% increase at the tidal boundary had a larger impact than SLR scenarios, which has clear implications for SLR in shelf sea tidal systems (and thus the tides propagating into an estuarine system).

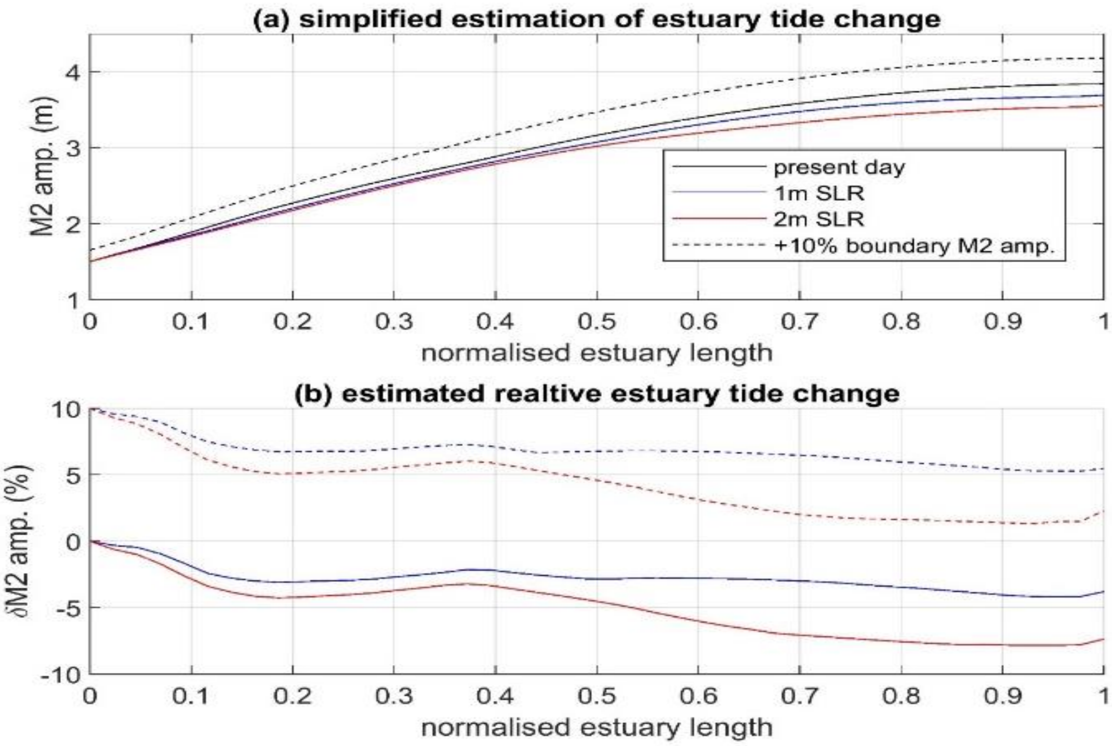

Fig. 5. Numerically simulated impact of tidal amplification on the major lunar semi-diurnal harmonic constituent (M2) in an idealised estuary, shown in panel (a), and the relative change to tidal amplification (δM2) shown in panel (b) for 1 m and 2 m of SLR – with the impact of a 10% change in the M2 amplitude at the estuary boundary shown with a dashed line.

It should be noted that uncertainties and assumptions in Fig. 5 render this result only suitable to demonstrate the potential impact of SLR in one idealised estuarine system (e.g., [52]). The interaction between SLR, tidal dynamics, and mobile bed sediments suggests that the geomorphic and tidal range resource response will be unique to every estuary. Nonetheless, simplified solutions of estuarine tidal dynamics have been shown to be useful [103] where freshwater discharge is limited [104] relative to the tidal range amplitude and anthropogenic activities do not change the estuary shape or depth [34, 105]. Hence, individual estuarine responses to SLR typically require location-specific modelling [52], particularly to understand the geomorphic response and interactions feedback loops of an estuarine system [106]. However, understanding and forward forecasting of geomorphic changes is extremely difficult as it requires the prediction of future meteorological events (i.e., floods, droughts) and their timing to accurately forecast bed geomorphic changes. Therefore, simplified analytical and numerical solutions (Fig. 4 and Fig. 5) as discussed herein are useful as they indicate that SLR is likely to change the present tidal range resource of estuaries.

3.3 Implications of altered tidal range for tidal range energy schemes

A growing body of literature indicates that SLR can induce significant changes to tidal dynamics across global estuaries [34, 35, 48], yet the resulting variations in the tidal energy resource remain largely unknown. It has been predicted that accelerating SLR will increase the tidal range in bays on the north coast of the Gulf of Mexico via increasing the cross-sectional area of the inlet and thereby, the tidal prism [55, 79]. SLR is likely to increase the tidal range within the Ems River estuary, although this increase would be smaller if overland flooding was permitted [107]. SLR may potentially increase the tidal range in the Delaware River estuary if adjacent lands were protected against flooding, due to a reduction in friction and an increase in convergence. Again, this range would decrease if neighbouring low-lying lands were allowed to be inundated, as more energy is dissipated over the shallow waters [53, 81]. In the Chesapeake Bay and its sub-estuaries, it is reported that SLR brings about an increase in the tidal range within the main stem of the estuary via an altered tidal resonance frequency and seaward shift of the amphidromic point [52]. SLR induces spatially unequal changes in tidal ranges of other tributaries so that six sub-estuaries (Potomac, James, York, Chester, Rappahannock, and Patuxent Rivers) generally experience tidal range amplification, and two sub-estuaries (Choptank and Patapsco Rivers) undergo tidal attenuation [52]. Further, the implications of SLR on the estuarine environment must be examined for the full tidal range (or tidal plane) as the high and low tide levels will often respond differently, invoking variable consequences [33]. For instance, where the tidal range is amplified, the low tide may not rise as far as the high tide, with the converse holding for those environments where the tidal range is attenuated, as illustrated in Fig. 6. In the Tamar River estuary in Australia, SLR is predicted to induce insignificant changes in the tidal range but it is predicted to reduce the flood dominated tidal asymmetry by up to 40% [54], which would naturally affect the power output of tidal turbines. As such, it is important to accurately predict the changes in tidal dynamics and associated tidal power in response to SLR.

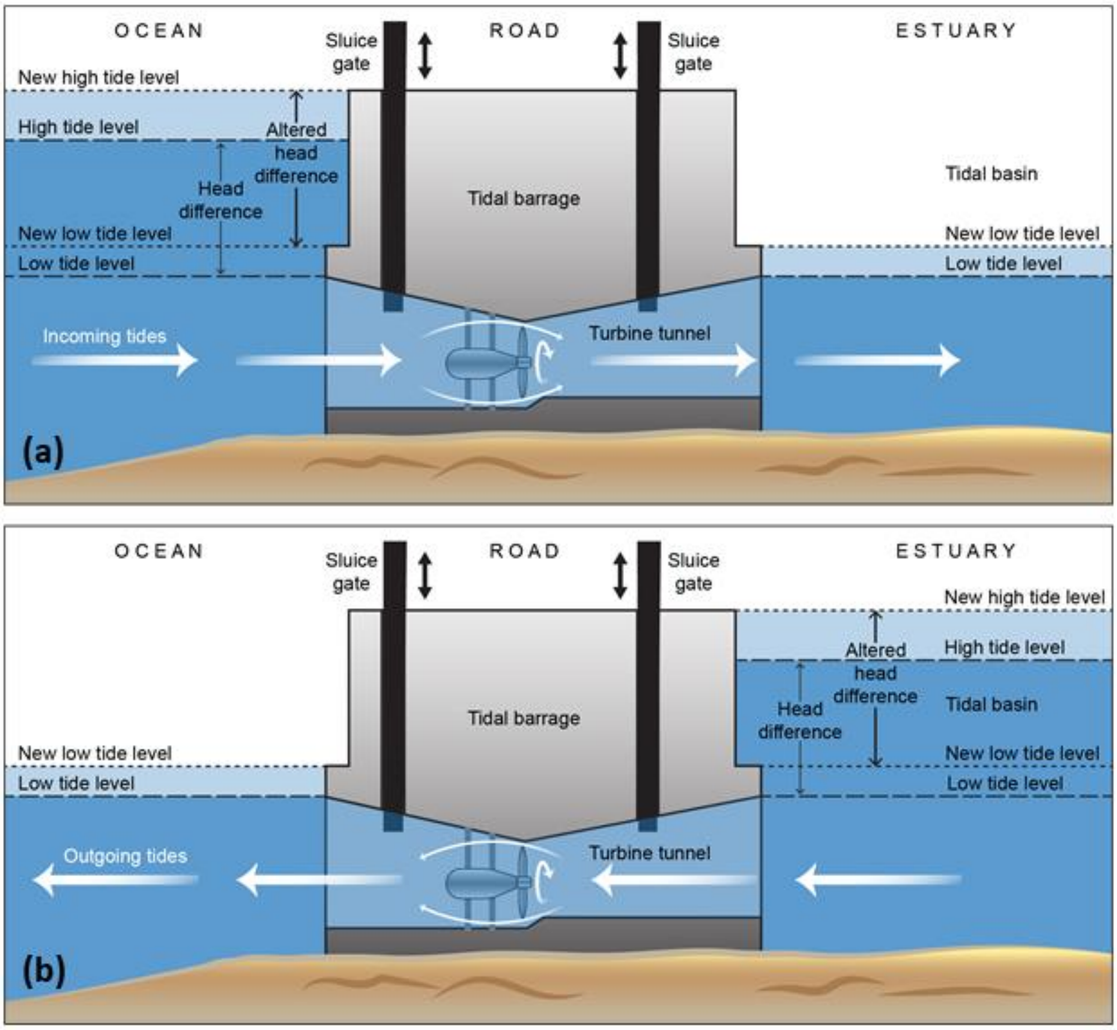

Fig. 6. (a) Operation of a tidal barrage with incoming (flood) tides or (b) outgoing(ebb) tides in present-day and future conditions. The high tide level may experience a larger amplification and a lower attenuation under SLR in comparison to low tide level.

4 Discussion

SLR is expected to affect the tidal prism, tidal range, or both, along with the location of amphidromic points, frictional effects, density forcing, tidal resonance characteristics and, subsequently, the geometry and bathymetry of the estuary. Depending on the estuary configuration, the tidal prism may increase or decrease under SLR [33, 55], such as in the case of Choctawhatchee Bay in the Gulf of Mexico, where SLR is predicted to increase the tidal prism whereas slightly reduce it in the nearby St Andrew Bay [55]. With respect to tidal range, tidal amplification has been predicted in a number of estuaries, often due to the presence of structures in the upper estuary that reflect the tidal wave or resonance phenomenon [74]. The geometry and bathymetry of the estuary may be modified by changes to the sediment transport dynamics, themselves caused by changes to the tidal flow patterns and/or asymmetry under SLR. In these circumstances, a complex feedback loop may exist over long timeframes.

The above changes caused by SLR, in turn, may affect the tidal stream velocity and therefore, the power density, as well as the location of the energy hotspots [49]. In relation to the changes to the tidal stream velocity, SLR is expected to increase the tidal stream velocities in many estuaries, even quite significantly (by 102% for a SLR of 2 m in the case of the Grand Bay, Gulf of Mexico), but decrease it in other cases due to the increased friction over low-lying, newly inundated areas (e.g., Chandeleur Islands area, also in the Gulf of Mexico region) [79].

With regards to the distribution of tidal energy hotspots, the sites with the greatest potential for tidal stream energy exploitation may shift or disappear as the sea level rises. It therefore follows that, in planning tidal stream farms, developers should consider not only the current situation but also future scenarios with different values of SLR. These values will correspond to different time points throughout the lifetime of the tidal stream farm and different climate change (SLR) scenarios. In practice, each SLR scenario should be investigated by means of a detailed hydrodynamic modelling study.

SLR has also been predicted to affect the tidal asymmetry [28, 46], which should be considered in designing the optimum site for a tidal stream farm. This is because tidal asymmetry is not beneficial to the exploitation of tidal stream power. Hotspots with limited or no asymmetry in the current situation may lose potential energy under SLR due to increased asymmetry. Conversely, hotspots where asymmetry is a problem at present may become more viable in the future, if and when SLR reduces the asymmetry [49, 50].

The previous paragraph was concerned with changes to the tidal asymmetry induced by SLR, without considering how the asymmetry affects the long-term sedimentary patterns of the estuary. As a reminder, flood and ebb dominated estuaries tend to move sediment landward and seaward, respectively. These sediment transport patterns will, over time, affect the shape of the estuary (e.g., estuary shape may shift from prismatic to converging or vice versa). A difficulty with making predictions in this respect is the lack of process-driven sediment dynamics model verification as it pertains to estimating the evolution of the estuarine system under SLR and varying environmental conditions over the tidal farm life cycle.

Geomorphic changes within an estuary, as driven by SLR, may also affect the tidal circulation and power density. It is important to note that these changes would be the result of various complex feedback loops. In short, SLR may initially affect the tidal prism and tidal range, which would subsequently affect the tidal current structure and tidal asymmetry, which would then affect the sediment transport, the estuary shape, and, eventually, the tidal power density.

Finally, the geomorphic configuration of an estuary is a key indicator of how fast the tidal circulation and power density of an estuary will respond to SLR. For example, short and/or converging estuaries respond faster to SLR than long and/or prismatic estuaries [78]. It follows that, if changes to the sediment transport patterns induced by SLR cause an estuary to evolve from a prismatic to a converging configuration, the effects of SLR on its tidal stream resource will be accelerated. A difficulty in estimating this factor – the possible shift in estuarine configuration, and the horizon of time over which it will occur – is the lack of validated models of sediment dynamics as it pertains to reliably predicting the evolution of estuarine systems under SLR over long periods of time, such as the life cycle of a tidal farm.

More immediate changes to the tidal power density may be expected to be caused by the direct effects of SLR (e.g., changes in depth and length). This line of thought leads logically to a hierarchy of factors influencing estuarine processes, with primary processes being modified directly by the SLR (e.g., tidal range, tidal prism, tidal currents), secondary processes (e.g., sediment transport patters) being affected by the SLR through the mediation of primary processes, tertiary processes (e.g., shift in estuary configuration) being modified by secondary factors, and the ongoing feedback loops between all processes.

In the case of tidal range energy, the effects of SLR are limited to a handful of specific estuaries and sub-estuaries. These effects have been shown to either increase or decrease the tidal range, depending on the particular estuary – or even particular sub-estuary – considered [52]. In both tidal stream and tidal range energy situations, the difficulty in estimating SLR impacts lies in applying generalised rules (or knowledge) to localised information. If available, tidal energy stakeholders will be able to connect the evolution of the tidal energy resource under SLR with the characteristics of an estuary. Such general rules may only be possible through comparative studies involving many estuary types. As such, future research in this area is recommended in view of the typical lifetime of tidal schemes, which in the case of tidal range may be as long as 120 years, given the large capital expenditures involved [86, 108]. Incidentally, the effects of SLR are relevant not only in estimating the resource over the lifetime of the schemes, but also in designing the structures themselves (the tidal barrage or tidal lagoon walls).

5 Conclusions

A review of research regarding tidal energy and SLR in estuaries was presented. The potential for tidal energy exploitation within an estuary – whether through tidal stream or tidal range schemes – is influenced by tidal dynamics and the geomorphic configuration (shape, bathymetry, bed roughness, etc.). The various mechanisms whereby the tidal energy resource may be affected by SLR have also been identified, including the changes in tidal prism, tidal range, tidal currents, tidal asymmetry, and sediment transport patterns.

Overall, based on the factors discussed above, SLR will induce nonlinear effects in an estuary which will depend on estuary shape and configuration. For instance, SLR may result in stronger or weaker tidal currents, depending on the estuary configuration. If large low-lying areas become inundated with SLR, the increase in friction may reduce the strength of the tidal currents in the estuary. As for tidal range, SLR may increase or decrease the range, depending on the shape and boundary conditions of the estuary, and the presence or absence of upstream structures capable of reflecting the tidal wave. It is apparent from this review that significant knowledge gaps remain as to the implications of SLR and the exploitation of tidal energy in estuaries, with different responses identified for different estuaries. Further, the difficulty in deriving general rules may be due to the lack of comparative studies across different regions and estuary types.

The influence of the various tidal factors identified may depend on their immediacy relative to SLR or, in other words, on how directly they are affected by SLR. As such, a hierarchy of factors may be established on these grounds. Primary factors are the tidal prism, tidal range, tidal currents, and tidal asymmetry, in which SLR has an immediate and direct role. Sediment transport is a secondary factor, given that it is affected by SLR indirectly, through its effects on primary factors. Finally, changes to the present-day estuarine configuration (e.g., planform changes) are a tertiary factor, given that they would result from the action of a secondary factor (sediment transport changes) over a longer time scale. To put it simply, primary factors are directly affected by SLR, which will influence and interact with secondary and tertiary factors through complex, interconnected feedback loops that will likely result in an influence across greater time scales.

In summary, SLR will have repercussions for available tidal energy resources as well as the distribution and location of potential energy hotspots. Changes to tidal dynamics due to SLR will have planning and management implications for existing and future tidal stream and tidal range energy schemes. A validated approach for assessing different climate change scenarios across the lifecycle of a project is currently absent but will hopefully be developed in future research as a decision-aid tool for policymakers and stakeholders.

6 Acknowledgments

Danial Khojasteh and Maryam Farzadkhoo are supported by UNSW Scientia PhD Scholarships.

Matthew Lewis wishes to acknowledge the support of the EPSRC METRIC project (EP/R034664/1).

7 References

[1] Pinto R, de Jonge VN, Neto JM, Domingos T, Marques JC, Patrício J. Towards a DPSIR driven integration of ecological value, water uses and ecosystem services for estuarine systems. Ocean & Coastal Management. 2013;72:64-79.

[2] O'Meara TA, Hillman JR, Thrush SF. Rising tides, cumulative impacts and cascading changes to estuarine ecosystem functions. Scientific Reports. 2017;7:10218.

[3] O'Higgins TG, Lago M, DeWitt TH. Ecosystem-based management, ecosystem services and aquatic biodiversity: theory, tools and applications. Switzerland: Springer Nature; 2020.

[4] Barbier EB, Hacker SD, Kennedy C, Koch EW, Stier AC, Silliman BR. The value of estuarine and coastal ecosystem services. Ecological monographs. 2011;81:169-93.

[5] Boerema A, Meire P. Management for estuarine ecosystem services: a review. Ecological Engineering. 2017;98:172-82.

[6] Marta-Almeida M, Cirano M, Soares CG, Lessa GC. A numerical tidal stream energy assessment study for Baía de Todos os Santos, Brazil. Renewable Energy. 2017;107:271-87.

[7] Savage C, Thrush SF, Lohrer AM, Hewitt JE. Ecosystem services transcend boundaries: estuaries provide resource subsidies and influence functional diversity in coastal benthic communities. PLoS One. 2012;7:e42708.

[8] Ross D. Introduction to oceanography. New York: HarperCollins College Publishers; 1995.

[9] Sheaves M, Baker R, Nagelkerken I, Connolly RM. True value of estuarine and coastal nurseries for fish: incorporating complexity and dynamics. Estuaries and Coasts. 2015;38:401-14.

[10] Díaz H, Rodrigues J, Soares CG. Preliminary assessment of a tidal test site on the Minho estuary. Renewable Energy. 2020;158:642-55.

[11] Xia J, Falconer RA, Lin B. Impact of different operating modes for a Severn Barrage on the tidal power and flood inundation in the Severn Estuary, UK. Applied Energy. 2010;87:2374-91.

[12] Vazquez A, Iglesias G. Device interactions in reducing the cost of tidal stream energy. Energy Conversion and Management. 2015;97:428-38.

[13] Ahmadian R, Olbert AI, Hartnett M, Falconer RA. Sea level rise in the Severn Estuary and Bristol Channel and impacts of a Severn Barrage. Computers & Geosciences. 2014;66:94-105.

[14] López A, Morán JL, Núñez LR, Somolinos JA. Study of a cost model of tidal energy farms in early design phases with parametrization and numerical values. Application to a second-generation device. Renewable and Sustainable Energy Reviews. 2020;117:109497.

[15] Lewis M, McNaughton J, Márquez-Dominguez C, Todeschini G, Togneri M, Masters I, et al. Power variability of tidal-stream energy and implications for electricity supply. Energy. 2019;183:1061-74.

[16] Garcia-Oliva M, Djordjević S, Tabor GR. The influence of channel geometry on tidal energy extraction in estuaries. Renewable Energy. 2017;101:514-25.

[17] Mestres M, Cerralbo P, Grifoll M, Sierra JP, Espino M. Modelling assessment of the tidal stream resource in the Ria of Ferrol (NW Spain) using a year-long simulation. Renewable energy. 2019;131:811-7.

[18] Qian P, Feng B, Liu H, Tian X, Si Y, Zhang D. Review on configuration and control methods of tidal current turbines. Renewable and Sustainable Energy Reviews. 2019;108:125-39.

[19] Vazquez A, Iglesias G. Capital costs in tidal stream energy projects–A spatial approach. Energy. 2016;107:215-26.

[20] Pacheco A, Gorbeña E, Plomaritis T, Garel E, Gonçalves J, Bentes L, et al. Deployment characterization of a floatable tidal energy converter on a tidal channel, Ria Formosa, Portugal. Energy. 2018;158:89-104.

[21] Khanjanpour MH, Javadi AA. Optimization of the hydrodynamic performance of a vertical Axis tidal (VAT) turbine using CFD-Taguchi approach. Energy Conversion and Management. 2020;222:113235.

[22] Pacheco A, Ferreira Ó, Carballo R, Iglesias G. Evaluation of the production of tidal stream energy in an inlet channel by coupling field data and numerical modelling. Energy. 2014;71:104-17.

[23] Ramos V, Carballo R, Álvarez M, Sánchez M, Iglesias G. A port towards energy self-sufficiency using tidal stream power. Energy. 2014;71:432-44.

[24] Sanchez M, Carballo R, Ramos V, Iglesias G. Energy production from tidal currents in an estuary: A comparative study of floating and bottom-fixed turbines. Energy. 2014;77:802-11.

[25] Ramos V, Carballo R, Sanchez M, Veigas M, Iglesias G. Tidal stream energy impacts on estuarine circulation. Energy Conversion and Management. 2014;80:137-49.

[26] Khojasteh D, Khojasteh D, Kamali R, Beyene A, Iglesias G. Assessment of renewable energy resources in Iran; with a focus on wave and tidal energy. Renewable and Sustainable Energy Reviews. 2018;81:2992-3005.

[27] Liu H-w, Ma S, Li W, Gu H-g, Lin Y-g, Sun X-j. A review on the development of tidal current energy in China. Renewable and sustainable energy reviews. 2011;15:1141-6.

[28] Radfar S, Panahi R, Javaherchi T, Filom S, Mazyaki AR. A comprehensive insight into tidal stream energy farms in Iran. Renewable and Sustainable Energy Reviews. 2017;79:323-38.

[29] Vazquez A, Iglesias G. A holistic method for selecting tidal stream energy hotspots under technical, economic and functional constraints. Energy Conversion and Management. 2016;117:420-30.

[30] Khojasteh D, Kamali R. Evaluation of wave energy absorption by heaving point absorbers at various hot spots in Iran seas. Energy. 2016;109:629-40.

[31] González-Caballín JM, Álvarez E, Guttiérrez-Trashorras AJ, Navarro-Manso A, Fernández J, Blanco E. Tidal current energy potential assessment by a two dimensional computational fluid dynamics model: The case of Avilés port (Spain). Energy Conversion and Management. 2016;119:239-45.

[32] Khojasteh D, Mousavi SM, Glamore W, Iglesias G. Wave energy status in Asia. Ocean Engineering. 2018;169:344-58.

[33] Khojasteh D, Hottinger S, Felder S, De Cesare G, Heimhuber V, Hanslow DJ, et al. Estuarine tidal response to sea level rise: The significance of entrance restriction. Estuarine, Coastal and Shelf Science. 2020;244:106941.

[34] Talke SA, Jay DA. Changing tides: The role of natural and anthropogenic factors. Annual Review of Marine Science. 2020;12:121-51.

[35] Khojasteh D, Glamore W, Heimhuber V, Felder S. Sea level rise impacts on estuarine dynamics: A review Science of The Total Environment. 2021;780:146470.

[36] Carballo R, Iglesias G, Castro A. Residual circulation in the Ria de Muros (NW Spain): a 3D numerical model study. Journal of Marine Systems. 2009;75:116-30.

[37] Iglesias G, Sánchez M, Carballo R, Fernández H. The TSE index – A new tool for selecting tidal stream sites in depth-limited regions. Renewable Energy. 2012;48:350-7.

[38] Angeloudis A, Kramer SC, Avdis A, Piggott MD. Optimising tidal range power plant operation. Applied energy. 2018;212:680-90.

[39] Xia J, Falconer RA, Lin B. Numerical model assessment of tidal stream energy resources in the Severn Estuary, UK. Proceedings of the Institution of Mechanical Engineers, Part A: Journal of Power and Energy. 2010;224:969-83.

[40] Sanchez M, Carballo R, Ramos V, Iglesias G. Floating vs. bottom-fixed turbines for tidal stream energy: A comparative impact assessment. Energy. 2014;72:691-701.

[41] Leuven JR, Pierik HJ, van der Vegt M, Bouma TJ, Kleinhans MG. Sea-level-rise-induced threats depend on the size of tide-influenced estuaries worldwide. Nature Climate Change. 2019;9:986-92.

[42] Sadat-Noori M, Rankin C, Rayner D, Heimhuber V, Gaston T, Drummond C, et al. Coastal wetlands can be saved from sea level rise by recreating past tidal regimes. Scientific reports. 2021;11:1-10.

[43] Rayner D, Glamore W, Grandquist L, Ruprecht J, Waddington K, Khojasteh D. Intertidal wetland vegetation dynamics under rising sea levels. Science of The Total Environment. 2021;766:144237.

[44] Oppenheimer M, Glavovic B, Hinkel J, van de Wal R, Magnan AK, Abd-Elgawad A, et al. Sea level rise and implications for low lying islands, coasts and communities. Intergovernmental Panel on Climate Change; 2019.

[45] Bamber JL, Oppenheimer M, Kopp RE, Aspinall WP, Cooke RM. Ice sheet contributions to future sea-level rise from structured expert judgment. Proceedings of the National Academy of Sciences. 2019;116:11195-200.

[46] Horton BP, Khan NS, Cahill N, Lee JS, Shaw TA, Garner AJ, et al. Estimating global mean sea-level rise and its uncertainties by 2100 and 2300 from an expert survey. npj Climate and Atmospheric Science. 2020;3:1-8.

[47] Sweet WWV, Kopp R, Weaver CP, Obeysekera J, Horton RM, Thieler ER, et al. Global and regional sea level rise scenarios for the United States. Maryland: National Oceanic and Atmospheric Administration; 2017.

[48] Haigh ID, Pickering MD, Green JM, Arbic BK, Arns A, Dangendorf S, et al. The Tides They Are A-Changin': A Comprehensive Review of Past and Future Nonastronomical Changes in Tides, Their Driving Mechanisms, and Future Implications. Reviews of Geophysics. 2020;58:e2018RG000636.

[49] Tang H, Kraatz S, Qu K, Chen G, Aboobaker N, Jiang C. High-resolution survey of tidal energy towards power generation and influence of sea-level-rise: A case study at coast of New Jersey, USA. Renewable and Sustainable Energy Reviews. 2014;32:960-82.

[50] Tang H, Qu K, Chen G, Kraatz S, Aboobaker N, Jiang C. Potential sites for tidal power generation: A thorough search at coast of New Jersey, USA. Renewable and Sustainable Energy Reviews. 2014;39:412-25.

[51] Chen W-B, Liu W-C. Assessing the influence of sea level rise on tidal power output and tidal energy dissipation near a channel. Renewable Energy. 2017;101:603-16.

[52] Du J, Shen J, Zhang YJ, Ye F, Liu Z, Wang Z, et al. Tidal response to sea-level rise in different types of estuaries: The Importance of Length, Bathymetry, and Geometry. Geophysical Research Letters. 2018;45:227-35.

[53] Lee SB, Li M, Zhang F. Impact of sea level rise on tidal range in Chesapeake and Delaware Bays. Journal of Geophysical Research: Oceans. 2017;122:3917-38.

[54] Palmer K, Watson C, Fischer A. Non-linear interactions between sea-level rise, tides, and geomorphic change in the Tamar Estuary, Australia. Estuarine, Coastal and Shelf Science. 2019;225:106247.

[55] Passeri DL, Hagen SC, Bilskie MV, Medeiros SC. On the significance of incorporating shoreline changes for evaluating coastal hydrodynamics under sea level rise scenarios. Natural Hazards. 2015;75:1599-617.

[56] Kresning B, Hashemi MR, Neill SP, Green JAM, Xue H. The impacts of tidal energy development and sea-level rise in the Gulf of Maine. Energy. 2019;187:115942.

[57] Lewis M, Neill SP, Robins PE, Hashemi MR. Resource assessment for future generations of tidal-stream energy arrays. Energy. 2015;83:403-15.

[58] Lewis MJ, Palmer T, Hashemi R, Robins P, Saulter A, Brown J, et al. Wave-tide interaction modulates nearshore wave height. Ocean Dynamics. 2019;69:367-84.

[59] Carballo R, Iglesias G, Castro A. Numerical model evaluation of tidal stream energy resources in the Ría de Muros (NW Spain). Renewable Energy. 2009;34:1517-24.

[60] Álvarez M, Carballo R, Ramos V, Iglesias G. An integrated approach for the planning of dredging operations in estuaries. Ocean Engineering. 2017;140:73-83.

[61] Kalogirou SA. Solar energy engineering: processes and systems. Second Edition ed: Elsevier; 2013.

[62] Adcock TA, Draper S, Willden RH, Vogel CR. The Fluid Mechanics of Tidal Stream Energy Conversion. Annual Review of Fluid Mechanics. 2021;53:287-310.

[63] Kadiri M, Ahmadian R, Bockelmann-Evans B, Rauen W, Falconer R. A review of the potential water quality impacts of tidal renewable energy systems. Renewable and sustainable energy reviews. 2012;16:329-41.

[64] Robins PE, Neill SP, Lewis MJ, Ward SL. Characterising the spatial and temporal variability of the tidal-stream energy resource over the northwest European shelf seas. Applied Energy. 2015;147:510-22.

[65] Tidal devices by European Marine Energy Centre (http://www.emec.org.uk/marine-energy/tidal-devices/) [Accessed: 15 February, 2021].

[66] Nachtane M, Tarfaoui M, Goda I, Rouway M. A review on the technologies, design considerations and numerical models of tidal current turbines. Renewable Energy. 2020;157:1274-88.

[67] Greaves D, Iglesias G. Wave and tidal energy: John Wiley & Sons; 2018.

[68] Sun J, Huang D. Numerical investigation on aerodynamic performance improvement of vertical-axis tidal turbine with super-hydrophobic surface. Ocean Engineering. 2020;217:107995.

[69] Kinsey T, Dumas G. Testing and analysis of an oscillating hydrofoils turbine concept. Fluids Engineering Division Summer Meeting2010. p. 9-22.

[70] Andersson J, Hellsmark H, Sandén BA. Shaping factors in the emergence of technological innovations: The case of tidal kite technology. Technological Forecasting and Social Change. 2018;132:191-208.

[71] De Swart H, Zimmerman J. Morphodynamics of tidal inlet systems. Annual review of fluid mechanics. 2009;41:203-29.

[72] Chen W, Chen K, Kuang C, Zhu DZ, He L, Mao X, et al. Influence of sea level rise on saline water intrusion in the Yangtze River Estuary, China. Applied Ocean Research. 2016;54:12-25.

[73] Vu D, Yamada T, Ishidaira H. Assessing the impact of sea level rise due to climate change on seawater intrusion in Mekong Delta, Vietnam. Water Science and Technology. 2018;77:1632-9.

[74] van Rijn LC. Analytical and numerical analysis of tides and salinities in estuaries; part I: tidal wave propagation in convergent estuaries. Ocean Dynamics. 2011;61:1719-41.

[75] Neill SP, Hashemi MR, Lewis MJ. The role of tidal asymmetry in characterizing the tidal energy resource of Orkney. Renewable Energy. 2014;68:337-50.

[76] Guo L, Wang ZB, Townend I, He Q. Quantification of tidal asymmetry and its nonstationary variations. Journal of Geophysical Research: Oceans. 2019;124:773-87.

[77] Zhang M, Townend I, Zhou Y, Cai H. Seasonal variation of river and tide energy in the Yangtze estuary, China. Earth Surface Processes and Landforms. 2016;41:98-116.

[78] Khojasteh D, Chen S, Felder S, Glamore W, Hashemi MR, Iglesias G. Tidal stream energy in estuaries under sea level rise. Energy. 2021.

[79] Passeri DL, Hagen SC, Plant NG, Bilskie MV, Medeiros SC, Alizad K. Tidal hydrodynamics under future sea level rise and coastal morphology in the Northern Gulf of Mexico. Earth's Future. 2016;4:159-76.

[80] Woodroffe CD, Rogers K, McKee KL, Lovelock CE, Mendelssohn I, Saintilan N. Mangrove sedimentation and response to relative sea-level rise. Annual Review of Marine Science. 2016;8:243-66.

[81] Ross AC, Najjar RG, Li M, Lee SB, Zhang F, Liu W. Fingerprints of Sea Level Rise on Changing Tides in the Chesapeake and Delaware Bays. Journal of Geophysical Research: Oceans. 2017;122:8102-25.

[82] van Maanen B, Sottolichio A. Hydro-and sediment dynamics in the Gironde estuary (France): sensitivity to seasonal variations in river inflow and sea level rise. Continental Shelf Research. 2018;165:37-50.

[83] Lewis MJ, Angeloudis A, Robins PE, Evans PS, Neill SP. Influence of storm surge on tidal range energy. Energy. 2017;122:25-36.

[84] Prandle D. Simple theory for designing tidal power schemes. Advances in water resources. 1984;7:21-7.

[85] Neill SP, Angeloudis A, Robins PE, Walkington I, Ward SL, Masters I, et al. Tidal range energy resource and optimization – Past perspectives and future challenges. Renewable Energy. 2018;127:763-78.

[86] Waters S, Aggidis G. Tidal range technologies and state of the art in review. Renewable and Sustainable Energy Reviews. 2016;59:514-29.

[87] Schindelegger M, Green JAM, Wilmes S-B, Haigh ID. Can We Model the Effect of Observed Sea Level Rise on Tides? Journal of Geophysical Research: Oceans. 2018;123:4593-609.

[88] Pelling HE, Mattias Green JA, Ward SL. Modelling tides and sea-level rise: To flood or not to flood. Ocean Modelling. 2013;63:21-9.

[89] Pickering MD, Horsburgh KJ, Blundell JR, Hirschi JJM, Nicholls RJ, Verlaan M, et al. The impact of future sea-level rise on the global tides. Continental Shelf Research. 2017;142:50-68.

[90] Pickering MD, Wells NC, Horsburgh KJ, Green JAM. The impact of future sea-level rise on the European Shelf tides. Continental Shelf Research. 2012;35:1-15.

[91] Woodworth PL, Teferle FN, Bingley RM, Shennan I, Williams SDP. Trends in UK mean sea level revisited. Geophysical Journal International. 2009;176:19-30.

[92] Khojasteh D, Glamore W, Heimhuber V, Hottinger S, Felder S. Implications of Tidal Resonance and Water Depth on Predicting Sea Level Rise in Estuaries. Australasia Coasts & Ports, . Hobart, Australia.2019.

[93] Garrett C. Tidal resonance in the Bay of Fundy and Gulf of Maine. Nature. 1972;238:441-3.

[94] Zhong L, Li M, Foreman MGG. Resonance and sea level variability in Chesapeake Bay. Continental Shelf Research. 2008;28:2565-73.

[95] Pelling HE, Mattias Green J. Sea level rise and tidal power plants in the Gulf of Maine. Journal of Geophysical Research: Oceans. 2013;118:2863-73.

[96] Pond S, Pickard GL. Introductory dynamical oceanography: Gulf Professional Publishing; 1983.

[97] Bonneton P, Bonneton N, Parisot J-P, Castelle B. Tidal bore dynamics in funnel-shaped estuaries. Journal of Geophysical Research: Oceans. 2015;120:923-41.

[98] Pugh DT. Tides, surges and mean sea-level (reprinted with corrections). Chichester, UK: John Wiley & Sons; 1996.

[99] Lanzoni S, D'Alpaos A. On funneling of tidal channels. Journal of Geophysical Research: Earth Surface. 2015;120:433-52.

[100] Friedrichs CT. Barotropic tides in channelized estuaries. Contemporary issues in estuarine physics. 2010;27:61.

[101] Ralston DK, Talke S, Geyer WR, Al-Zubaidi HAM, Sommerfield CK. Bigger Tides, Less Flooding: Effects of Dredging on Barotropic Dynamics in a Highly Modified Estuary. Journal of Geophysical Research: Oceans. 2019;124:196-211.

[102] Neill SP, Litt EJ, Couch SJ, Davies AG. The impact of tidal stream turbines on large-scale sediment dynamics. Renewable Energy. 2009;34:2803-12.

[103] Zhang EF, Savenije HHG, Chen SL, Mao XH. An analytical solution for tidal propagation in the Yangtze Estuary, China. Hydrol Earth Syst Sci. 2012;16:3327-39.

[104] Prandle D, Lane A. Sensitivity of estuaries to sea level rise: Vulnerability indices. Estuarine, Coastal and Shelf Science. 2015;160:60-8.

[105] Prandle D. How tides and river flows determine estuarine bathymetries. Progress in Oceanography. 2004;61:1-26.

[106] Todeschini I, Toffolon M, Tubino M. Long-term morphological evolution of funnel-shape tide-dominated estuaries. Journal of Geophysical Research: Oceans. 2008;113.

[107] Ensing E, de Swart HE, Schuttelaars HM. Sensitivity of tidal motion in well-mixed estuaries to cross-sectional shape, deepening, and sea level rise. Ocean Dynamics. 2015;65:933-50.

[108] Roberts A, Thomas B, Sewell P, Khan Z, Balmain S, Gillman J. Current tidal power technologies and their suitability for applications in coastal and marine areas. Journal of Ocean Engineering and Marine Energy. 2016;2:227-45.